Journal of Thermal Analysis and Calorimetry, Vol. 73 (2003) 3–15

STUDY OF THE REDUCTION OF TUNGSTEN TRIOXIDE DOPED WITH MCl (*M*=Li, Na, K)

G. K. Schwenke[1], *M. Feist*[2] *and H.-J. Lunk*[1*]

[1]OSRAM Sylvania Chemical and Metallurgical Products, Towanda, PA, USA
[2]Institut für Chemie, Humboldt University Berlin, Germany

(Received May 14, 2002; in revised form October 31, 2002)

Abstract

Thermodynamic calculations predict the formation of hydrochloric acid gas and alkali tungstates during hydrogen reduction of WO_3 doped with alkali chlorides MCl (*M*=Li, Na, K). The formation of HCl was proved experimentally by simultaneously coupled TG-MS measurements from RT to 1200ºC.

The formation of HCl is the result of the reaction between MCl, WO_3 and water. Ubiquitous traces of moisture in the gas are sufficient for reaction according to $WO_3+(2+2n)MCl+(1+n)H_2O \rightarrow M_{2+2n}WO_{4+n}+(2+2n)HCl$ (n=0, 1, 2).

Laboratory reduction tests showed that the formed tungstates differ. NaCl and KCl form monotungstates (n=0), while LiCl produces more lithium-rich compounds (n=1, 2). Temperature and humidity, among other process factors, control subsequent reduction of the tungstates to metals.

Keywords: alkali chlorides, reduction, TG-MS coupling, thermodynamic calculation, WO_3

Introduction

The doping of tungsten trioxide, WO_3, with alkali metals and the subsequent hydrogen reduction of the doped powder is part and parcel of producing coarse tungsten powder [1]. Hundreds of parts per million alkali chlorides are commonly added, yet after reduction, the tungsten powders contain only traces of the added dopants. It is of eminent theoretical and practical interest to elucidate if the chlorides evaporate in the form of $(MCl)_n$ (n=1, 2), as HCl, or according to both routes. Thermodynamic calculations and experimental work have been undertaken to answer the question.

Thermodynamic calculations

Thermodynamic calculations can predict how chlorides are removed from the system as WO_3(MCl) blends are reduced in hydrogen. Alkali chlorides can react with tungsten, its oxides, water, and/or hydrogen. Possible products include hydrochloric acid,

* Author for correspondence: E-mail: hans-joachim.lunk@sylvania.com

1388–6150/2003/ $ 20.00
Akadémiai Kiadó, Budapest

alkali tungstates, tungsten bronzes, hydroxides, oxides and the metals themselves. Or the alkali chlorides can simply evaporate. The formation of alkali hydrides, tungsten chlorides, and tungsten oxychlorides is unlikely under the conditions studied.

The approach was to examine the stability of selected compounds over a range of temperatures and dew points, then compute equilibrium partial pressures of chlorine-containing species from several potential reactions. Whichever reaction generates the highest vapor pressure is assumed to be the path by which chloride is removed. Calculations span temperatures from 25 to 1727°C (298 to 2000 K) and dew points from –47 to 25°C (gas moisture contents of 50 vpm to 3.2 vol.%). Thermodynamic data comes from four sources [2–5]. Most authors report coefficients for a Shomate equation, which can be integrated to yield an expression for Gibbs free energy. Vapor pressure data was calculated with an Antoine-equation fit to tabular data [6].

Figure 1 plots the WO_3(NaCl) system under a hydrogen atmosphere with a dew point (*DP*) of 25°C. Under these moist conditions, WO_3 will give way to WO_2 as the stable phase at 202°C, and W will supplant WO_2 at 417°C. Temperatures are too low for two so-called tungsten sub-oxides – $W_{20}O_{58}$ and $W_{18}O_{49}$ – to be thermodynamically stable. Over this entire temperature range, HCl from formation of cubic sodium tungsten bronze has the highest vapor pressure of any chlorine-containing compound. Three reactions are involved:

$$WO_3+0.794NaCl+0.397H_2=Na_{0.794}WO_3+0.794HCl \quad (1)$$

$$WO_2+0.794NaCl+H_2O=Na_{0.794}WO_3+0.794HCl+0.603H_2 \quad (2)$$

$$W+0.794NaCl+3H_2O=Na_{0.794}WO_3+0.794HCl+2.603H_2 \quad (3)$$

Evolution of HCl accompanying bronze formation dominates until 552°C, at which point, sodium chloride will form sodium tungstate instead:

$$W+2NaCl+4H_2O=Na_2WO_4+2HCl+3H_2 \quad (4)$$

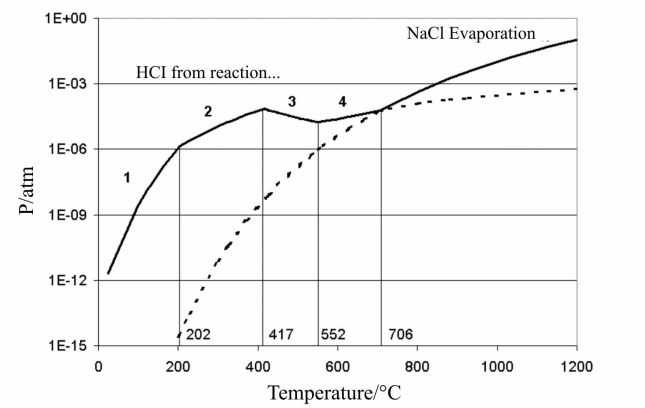

Fig. 1 Equilibrium pressures of HCl and NaCl over WO_3(NaCl) at T_{DP}=25°C

This reaction remains valid to the upper temperature limit of the thermodynamic data, but at 706°C, the vapor pressure of NaCl surpasses the pressure of HCl generated by reaction (4). Vertical lines in Fig. 1 denote temperatures where the dominant reactions shift.

Note that $Na_{0.794}WO_3$ and Na_2WO_4 remain stable under conditions where WO_2 will reduce to W. Therein lies the reason sodium is an effective dopant: it retards reduction until high temperature, enabling growth of tungsten crystals by chemical vapor transport via $WO_2(OH)_2$ [7]. At sufficiently high temperature, Na_2WO_4 will reduce to W(*s*) and Na(*g*), but a dew point of 25°C requires a temperature well in excess of 1227°C (the limit of the thermodynamic data for Na_2WO_4).

If the same NaCl-doped WO_3 is reduced in dry hydrogen (–40°C dew point), reduction will occur at distinctly lower temperatures, and HCl formation will be suppressed. WO_2 is stable from room temperature to 127°C, at which point W should form. Reaction (1) is no longer relevant, and reactions (2) through (4) all contain H_2O as a reactant. Le Châtelier's principle explains lower HCl pressures, but NaCl evaporation is unaffected. As a result, the HCl to NaCl shift temperature falls to 320°C.

Dilution of the hydrogen (such as adding nitrogen to it) also affects the temperatures of the shifts. Compared to pure H_2, a hydrogen/nitrogen mixture with the same dew point is a less powerful reducing agent. Consequently, reduction requires higher temperatures, and reactions (1) and (2) are more important. In addition, a lower hydrogen pressure displaces equilibrium in reactions (2) through (4) to the right, favoring HCl formation.

The WO_3(LiCl) and WO_3(KCl) systems can be analyzed in a similar manner, except for a lack of data for lithium or potassium tungsten bronzes. Lithium and potassium chlorides can react with tungsten and its oxides to form corresponding monotungstates. Potassium monotungstate reduces to W(*s*) and K(*g*), just as sodium tungstate does. However, lithium tungstate will only reduce partially, leaving LiOH(*s*) or Li_2O(*s*) along with W(*s*). Figure 2 plots the temperatures of HCl to MCl (*M*=Li, Na, or K) shifts in these systems as functions of dew point.

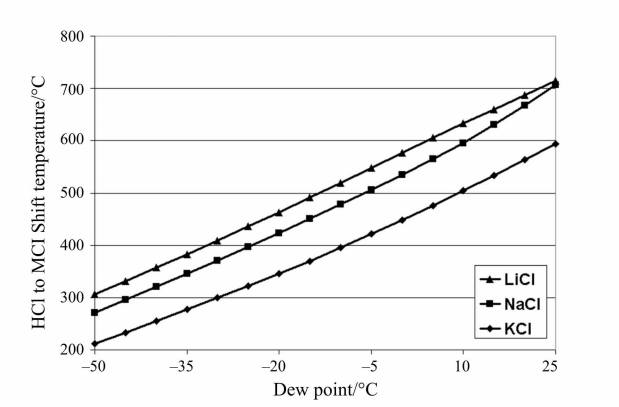

Fig. 2 HCl to MCl (*M*=Li, Na, K) shift temperatures *vs.* dew point

The dew point is critical to whether alkali chlorides first react or evaporate. Shift temperatures in all three systems climb by about 400°C as the dew point rises from –50 to 25°C. The importance of humidity cannot be overstated. Under dry conditions, evaporation of MCl is more important; under wet conditions, HCl formation is. Another conclusion is that potassium chloride is the most likely to evaporate. At any dew point shown, KCl evaporation will surpass HCl from K_2WO_4 formation at a lower temperature than in the sodium or lithium systems. Lithium chloride is the least likely to evaporate. Sodium chloride is intermediate but closer to LiCl.

Though strictly valid only for closed systems at equilibrium, these thermodynamic calculations certainly provide a basis for understanding. They illustrate trends, such as the effect of humidity and differences between the three alkali chlorides. Results are not meant to be interpreted quantitatively. The important point is that alkali chlorides are likely to react and form HCl, not that they will do so at a precise temperature and dew point. One other limitation of the thermodynamic calculations is that not all possible compounds are considered – just those with published free energies. In addition to tungsten bronzes, tungsten is known to form more complex oxides, such as $M_2O{\cdot}mWO_3$ (m=2–8) and $nM_2O{\cdot}WO_3$ (n=2, 3). Whenever these phases are more stable than the corresponding mixtures of M_2O, WO_3, and/or sub-oxides, their formation (and HCl generation) is favored. Their roles cannot be calculated, but they could be significant. In experiments and especially under manufacturing conditions, kinetic factors impact the relative importance of HCl formation *vs*. MCl evaporation. Reaction rates are functions of boatload, gas flow, stoke rate, and other process factors. Both routes of chloride removal operate in parallel, and their simultaneous contributions remove chlorine faster than either single path. Experimental work was needed to answer the question of whether chlorides first react or evaporate.

Experimental

Thermodynamic calculations were checked by performing experiments. The starting material, tungsten trioxide, was produced by calcining OSRAM Sylvania's ammonium paratungstate tetrahydrate, $(NH_4)_{10}[H_2W_{12}O_{42}]{\cdot}4H_2O$, in air, yielding the monoclinic modification of WO_3. The oxide gave a drying loss of 0.01%; aluminum (2 ppm) was the only impurity detected. It has an average particle size of 16 μm, measured by Fisher Sub Sieve Sizer (FSSS), and a bimodal particle size distribution with a median size of 15 μm (as measured by a Leeds & Northrup Microtrac X100 particle size analyzer). Alkali chloride salts were obtained from Aldrich (LiCl) and Mallinckrodt (NaCl and KCl). They were milled in porcelain jars prior to blending.

Three 5 kg batches of doped tungsten trioxide were prepared. They were doped with 1.51 LiCl, 2.08 NaCl, and 2.65% KCl. These amounts are much higher than common industrial doping additions. They were selected to facilitate detection of mass losses, gaseous species, and chemical changes. They have the same molar concentration (35.5 mmol MCl per 100 g blend, which equals 1.26% Cl^- in each sample). We used a stepwise procedure, first adding the entire quantity of the milled chloride

to a small amount of WO_3, then distributing it into more undoped oxide. Five installments were rolled in progressively larger plastic bottles for an hour each. Samples for TG-MS measurements were obtained by chute-splitting the resulting blends. In the case of WO_3 doped with LiCl, special precautions were applied because of the hygroscopicity of the salt. The lithium chloride was dried overnight at 140°C prior to weighing and blending. The crucible filled with the doped oxide was kept in a desiccator over phosphorus pentoxide over several days, and then taken out immediately before measurement.

Reduction was studied by simultaneously coupled TG-MS measurements. A Netzsch STA 409 C thermoanalyzer Skimmer® system, equipped with a Balzers mass spectrometer QMG 422, was used to record the thermoanalytical curves (T, TG, DTG) together with the ionic current (IC) curves in the multiple ion detection (MID) mode. A TG sample carrier system with corundum plate crucibles (17 mm diameter) and Pt/PtRh10 thermocouples was used. Purge gas flowed over the samples at a constant rate of 70 mL min^{-1}. Two gas atmospheres were used: 5% H_2 in N_2 and pure N_2. Both had dew points below –50°C. Samples, 69–74 mg each, were heated to 1200°C at a ramp rate of 10 K min^{-1}, and then cooled. Thermal stress considerations for the Skimmer system require a controlled cooling segment (20 K min^{-1}) down to 800°C. Consequently, for several runs, reaction continued into the cooling segment. In one case (Fig. 5), the TG curve, including the mass loss values, is plotted *vs*. time. IC curves are generally temperature-scaled. The raw data have been evaluated utilizing the manufacturer's PROTEUS® software (v. 4.1) without further data treatment, such as smoothing. Following the international recommendation [8], for each peak, three temperatures were determined, namely the initial (T_i), the extrapolated onset (T_{on}^{ex}), and the peak temperature (T_P).

Because of sample size limitations in the TG/DTG/MS experiments, supplemental laboratory-scale reduction tests were performed in a programmable 2.5" diameter Lindberg® furnace, using 5 and 15 g samples. They were reduced in dry (dew point –45°C) and wet (dew point ~0°C) hydrogen, using a constant ramp of 10 K min^{-1} and a final 15 min hold at 950 or 1100°C. The reduced powders and their water extracts were analyzed by standard methods, including mass spectroscopy, atomic absorption, and pH measurement.

TG-MS measurements

Tables 1.1 and 1.3 summarize the results of the quantitative TG evaluation of all four systems investigated. See sections 4.1 through 4.3 for detailed discussion. Table 1.2 compiles the theoretical mass losses for various reaction paths.

The base line shift of the IC signals (e.g. *m/z* 17, 18 in Figs 3 and 4) is characteristic of the Skimmer® system where the gas sampling system and the sample holder have the same temperatures, thus avoiding condensation phenomena. Consequently, the MS signal becomes temperature-dependent, and increasing baseline IC intensities at higher temperatures do not indicate generation of gas from the sample.

Table 1 Observations from TG-MS experiments and theoretical calculcations

Table 1.1 Mass losses/% measured by TG-MS

Stages	Undoped WO_3	WO_3(LiCl)	WO_3(NaCl)	WO_3(KCl)
Loss of adsorbed H_2O	0.12	traces	0.14	0.03
HCl formation	n/a	0.97	1.28	1.27
Reduction of WO_3				
Step 1	1.98	6.33	1.31	1.45
Step 2	4.98		4.38	4.59
Step 3	13.72	13.34	13.03	13.13
Reduction of M_2WO_4	n/a		0.48	1.98
Subtotal	20.68	20.64	20.48	22.42
Total	20.80	20.64	20.62	22.45

Table 1.2 Sample compositions and theoretical mass losses

Stages	Undoped WO_3	WO_3(LiCl)	WO_3(NaCl)	WO_3(KCl)
M/mass%	0	0.25	0.82	1.39
Cl/mass%	0	1.26	1.26	1.26
MCl/mass%	0	1.51	2.08	2.65
		Mass loss/% for...		
Reduction of WO_3 to W	20.70	20.39	20.27	20.15
Plus loss of Cl	n/a	21.65	21.53	21.41
Plus loss of M	n/a	21.90	22.35	22.80
–or–				
Plus M forming M_2WO_4+HCl	n/a	20.53	20.39	20.28
–or–				
Plus M forming M_4WO_5+HCl	n/a	20.93	20.82	20.70
–or–				
Plus M forming M_6WO_6+HCl	n/a	21.07	20.96	20.85

Undoped WO_3

Figure 3 shows the TG-MS curves for the reduction of undoped WO_3. According to the TG curve, the reduction starts at T_i=579°C, and it is characterized by three steps, which widely overlap each other. Therefore, only the beginning and the end of the reaction can be stated unequivocally, and the intermediate mass losses yield only qualitative informa-

Table 1.3 Temperatures/°C for stages of reduction measured by TG-MS

Stages	Undoped WO_3		WO_3(LiCl)		WO_3(NaCl)		WO_3(KCl)	
	T_i	T_p	T_i	T_p	T_i	T_p	T_i	T_p
Loss of adsorbed H_2O	25–580		100–600		70–550		60–480	
HCl formation (IC curve)	n/a		347	536	506	669	451	642
Reduction of WO_3 (TG curve)								
Step 1	579	773	720	893	706	747	672	744
Step 2	785	838			780	871	776	866
Step 3	885	1048	914	1038	905	1065	891	1026
Reduction of M_2WO_4	n/a	n/a	–	–	1120	1170	1062	1137

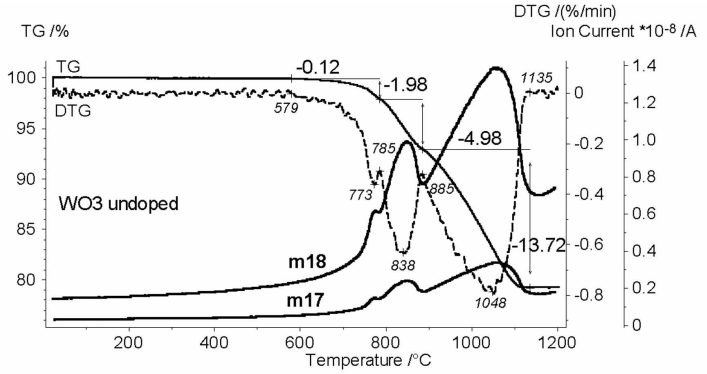

Fig. 3 TG and DTG curves for undoped WO_3 reduction with the IC curves for *m/z* 17 (OH^+) and 18 (H_2O^+) in 5% H_2/95% N_2. Relevant temperatures describing the beginning/overlapping of the TG steps are marked (+) on the TG and DTG curves

tion. In the same way, the peak temperatures $\{T_P\}$ being influenced by the sample mass, among other factors, are helpful for comparison with each other, but they are of limited value for more general conclusions. Nevertheless, the coincidence of the DTG and IC extrema provides an excellent description of the reduction process.

The three detectable steps represent the following reduction stages [9]:
$WO_3 \rightarrow W_{18}O_{49}$ (via $W_{20}O_{58}$) with a calculated mass loss of 1.93%,
$W_{18}O_{49} \rightarrow WO_2$ (calculated mass loss 4.97%),
$WO_2 \rightarrow W$ (calculated mass loss 13.80%).

NaCl- and KCl-doped WO_3

The same three steps as in the undoped sample occur in the systems WO_3(NaCl) and WO_3(KCl), Figs 4 and 5. Two additional TG steps occur before reduction of tungsten

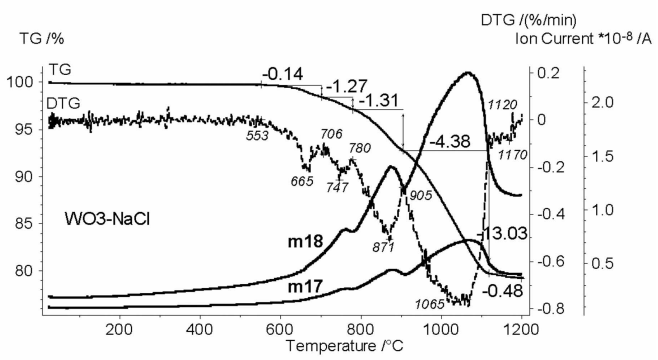

Fig. 4 TG and DTG curves for WO_3 (2.08% NaCl) reduction with the IC curves for *m/z* 17 (OH^+) and 18 (H_2O^+); *cf.* explanations to Fig. 3

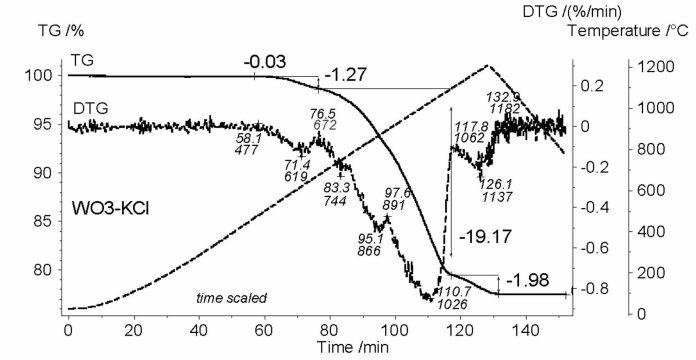

Fig. 5 TG and DTG curves for WO_3 (2.65% KCl) reduction. Note that the final plateau of the TG curve is reached only during cool-down which requires the time-scaled plot. Consequently, marker positions are given in min and temperature values are added below the time labels. The value for T_i (HCl) determined by TG amounts to 477°C whereas MS yields 451°C (curves not shown)

oxides. The first step is minor; it reflects the release of adsorbed water. The second step is due to the reaction of the dopants.

Figure 6 plots more IC curves for system WO_3(NaCl), those for *m/z* 35 ($^{35}Cl^+$), 36 ($H^{35}Cl^+$) and 38 ($H^{37}Cl^+$). It clearly proves that chlorine is liberated in the form of HCl and that its release is practically finished in a very early stage of the reduction process.

The system WO_3(KCl) results in a release of HCl similar to that for WO_3(NaCl). See Table 1 for details.

LiCl-doped WO_3

The system WO_3(LiCl), Fig. 7, exhibits a TG curve with a shape different from those in Figs 4 and 5. Reduction of WO_3(LiCl) is characterized by two WO_3 reduction steps instead of three. The peak temperatures and their relative intensities are different as well.

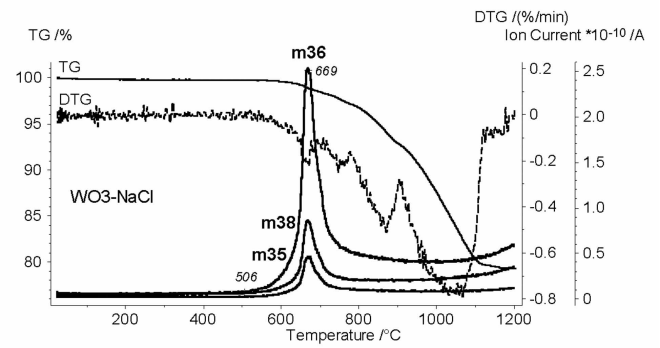

Fig. 6 TG, DTG and IC curves for WO_3 (2.08% NaCl) reduction, *m/z* 35 ($^{35}Cl^+$), 36 ($H^{35}Cl^+$) and 38 ($H^{37}Cl^+$) with marked onset and peak temperatures for the HCl

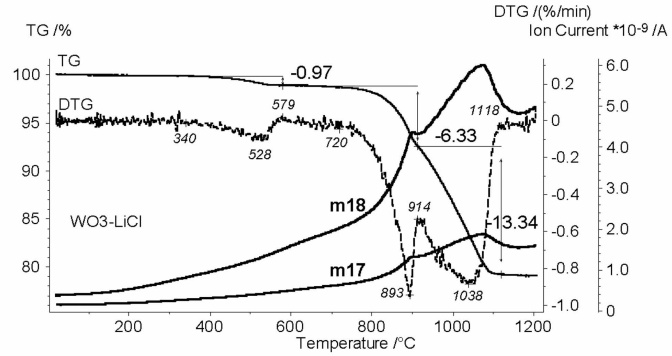

Fig. 7 TG and DTG curves for WO_3 (1.53% LiCl) reduction with the IC curves for *m/z* 17 (OH^+) and 18 (H_2O^+); cf. explanations to Fig. 3

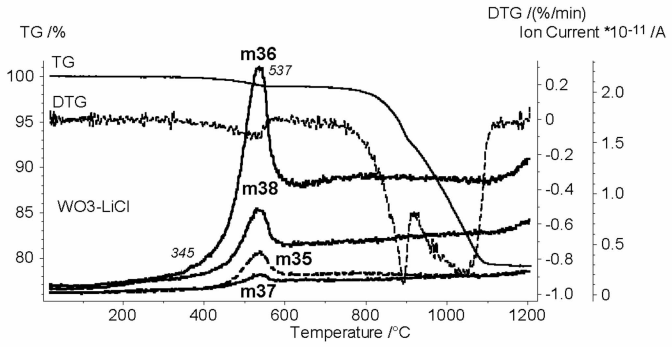

Fig. 8 IC curves for WO_3 (1.51% LiCl) reduction, *m/z* 35 ($^{35}Cl^+$), 36 ($H^{35}Cl^+$) and 38 ($H^{37}Cl^+$). Note that the absolute level of the enhanced background above 570°C is not greater than for WO_3(NaCl) (Fig. 6)

The release of HCl from WO_3(LiCl) starts at considerably lower temperatures (T_i=347, T_P =536°C) than in the case of NaCl- and KCl-doped WO_3 samples, and the HCl IC signal (Fig. 8) is broader.

Laboratory reduction experiments

Analytical data from a series of laboratory-scale reduction experiments is represented in Table 2. Under the experimental conditions used, none of the reduced powders contains any detectable chloride (<1 ppm). While the whole amount of Cl^- had left the solid, in some samples, substantial quantities of alkali metal remained.

Either evaporation of MCl or reduction of tungstates formed from it can result in the loss of metal and chloride. However, only tungstate formation can explain residual alkali metal without chloride. Our challenge was to 'catch' the tungstate after its formation but before its reduction. Larger sample sizes and wet hydrogen will retard reduction of the tungstates.

The reduction of 5 g samples in dry hydrogen at 950ºC illustrates the different behavior of the systems studied. In the case of LiCl-doped WO_3, the entire amount of added lithium was found in the reduced tungsten powder. Under the same conditions, the system WO_3(KCl) lost more than 95% of its potassium, and the system WO_3(NaCl) lost almost 100% of its sodium. For the system WO_3(LiCl), a moderate loss of about 30% of the added lithium required a final reduction temperature of 1100ºC.

Table 2 Reduction of MCl-doped WO_3 (*M*=Li, Na, K) with dry and wet hydrogen; ramp 10 K min^{-1}, final 15 min hold at 950 or 1100°C

Reduction conditions	Tungsten powder	Aqueous extraction			
	M/ppm	pH (325 g L^{-1})	*M*/ppm	W/ppm	Mole ratio *M*:W
1.51% LiCl; 3.100 ppm Li, 15.900 ppm Cl (based on W)					
5 g; 950°C; dry	3.500	–	3.240	16.000	5.4:1
5 g; 1100°C dry	2.000	–	1.950	10.300	5.0:1
5 g; 950°C; wet	3.500	–	3.380	20.700	4.3:1
15 g; 950°C; wet	3.600	11.6	3.360	19.800	4.5:1
2.08% NaCl: 10.300 ppm Na, 15.900 ppm Cl (based on W)					
5 g; 950°C; dry	34	–	18	620	n/a[a)]
5 g; 950°C; wet	7.400	–	7.870	33.100	1.9:1
15 g; 950°C; wet	10.000	7.6	9.440	40.900	1.8:1
2.65% KCl: 17.500 ppm K, 15.900 ppm Cl (based on W)					
5 g; 950°C; dry	519	–	469	1.310	1.7:1
5 g; 950°C; wet	17.500	–	16.200	38.400	2.0:1
15 g; 950°C; wet	17.300	7.8	16.100	35.600	2.1:1

[a)]Because of the small amounts Na and W detected, the mole ratio is not reliable.

The reduction of 5 g samples in wet hydrogen at 950ºC produced tungsten powders with 100% Li and K, but only about 70% Na remaining. The reduction of 15 g samples in wet hydrogen did not differentiate alkali metal retention in the three systems; in each case the full amount remained.

In addition to direct analysis of the reduced tungsten powders, all the samples were extracted with de-ionized water. Measurement of the extracts' pH values and determination of alkali metal and tungsten concentrations gives valuable information about the systems (Table 2). Virtually the entire amount of alkali metal found in all three tungsten powders is extractable. The mole ratio Li:W reveals that the lithium tungstates Li_4WO_5 and Li_6WO_6 are formed in the system WO_3(LiCl). Their complete hydrolytic decomposition during extraction results in the high pH. The two other alkali metals lead to their respective monotungstates, M_2WO_4, both highly soluble in water, producing a weakly alkaline solution with a mole ratio of 2 M:1 W and a moderately alkaline pH.

Discussion

Under the experimental conditions in the thermoanalyzer (dew point <–50°C, small sample size of 70 mg, maximum temperature 1200ºC), the reaction leads to the formation of Na_2WO_4, which is only partially reduced to Na and W. Complete reduction of Na_2WO_4 would result in a mass loss of 1.96% (=22.35–20.39%), but Table 1.1 shows only 0.48% (step 4). Thus, we would expect roughly one fourth of the Na_2WO_4 to have reduced. The system WO_3(KCl) loses its entire amount of potassium via reduction of K_2WO_4. The theoretical mass loss of 2.52% (=2.80–20.28%) is close to the 1.98% loss listed in Table 1.1.

The system WO_3(LiCl) behaves differently, not exhibiting an additional reduction step at all. Obviously, the lithium tungstates formed are stable under the reduction conditions used. The amount of chloride detected, 0.97%, is a little low compared to the 1.26% theoretical content, which was experimentally confirmed for the other two systems.

Reduction of WO_3 is not required for the formation of HCl, though it can supply H_2O if other sources are not available. The reaction between WO_3, MCl and H_2O according to

$$WO_3+(2+2n)MCl+(1+n)H_2O \rightarrow M_{2+2n}WO_{4+n}+(2+2n)HCl \quad (5)$$

(n=0, 1, 2) starts at relatively low temperature (T_i=347, 506 and 451ºC for LiCl, NaCl, and KCl, respectively), and it is practically finished in a very early stage of the reduction process. The corresponding peak temperatures lie below the initial temperatures of the WO_3 reduction: 536 (T_p for HCl) *vs*. 736ºC (T_i for reduction) for LiCl, 669 *vs*. 706ºC for NaCl, and 642 *vs.* 672ºC for KCl (Table 1.3). The ubiquitous traces of moisture (30 vpm) in the gas mixture used are sufficient for the observed displacement reaction. The highly volatile hydrochloric acid is being displaced from its salts by a non-volatile acid, in our case the acidic oxide WO_3. This reaction has been proved by a separate measurement of the system WO_3(KCl) in pure nitrogen yielding a quite analogous curve shape as the test

in 5% H_2/95% N_2. The only difference is that under inert conditions, the HCl release starts at somewhat higher temperature (T_i =470, T_P=684°C) than in the presence of hydrogen (T_i=451, T_P=642°C).

For all three systems investigated, no release whatsoever of alkali metal-containing species, such as *M*, MCl, $(MCl)_2$, or MOH, could be observed. While the lack of gaseous MCl supports the HCl pathway for chloride elimination, the non-detection of any *M* requires an explanation. Because of their reactivity, alkali metals and their oxides are difficult to detect by MS. For example, potassium oxide could not be detected by using three different diaphragm materials (steel, corundum, glassy carbon) in the Skimmer® system [10].

Under the conditions of our laboratory experiments, the hydrogen reduction of the system WO_3(LiCl) leads to W+Li_4WO_5 /Li_6WO_6, whereas under analogous conditions the monotungstates Na_2WO_4 and K_2WO_4 are formed. These monotungstates can be fully reduced in dry H_2 according to

$$M_2WO_4+4H_2 \rightarrow 2M+W+4H_2O \quad (6)$$

Reaction (6) explains the loss of sodium and potassium at higher temperatures (Tables 1.1. and 1.3). Thermodynamic calculations predict that under dry (dew point –50°C) conditions, Na_2WO_4 and K_2WO_4 will reduce at 1090 and 1078°C (both below the maximum temperature attained in the TG/DTG/MS) in an atmosphere containing 5% H_2. Undiluted, the same dry hydrogen can reduce them at much lower temperatures, namely 838 and 856°C, respectively. The reducibility of K_2WO_4 in dry hydrogen at temperatures (as low as 850°C) was proven experimentally [11]. The reduction of alkali monotungstates under wet conditions demands distinctly higher temperatures.

Obviously, the lithium tungstates Li_4WO_5 and Li_6WO_6 are much more reduction-resistant than the sodium and potassium monotungstates, which explains the observed differences. Unfortunately, thermodynamic data for these lithium tungstates could not be found.

Conclusions

Thermodynamic calculations predict the formation of hydrochloric acid gas during the hydrogen reduction of WO_3 doped with alkali chlorides. The dew point is critical in determining whether alkali chlorides first react or evaporate, and LiCl is the most likely to form HCl. The formation of HCl was proved experimentally by simultaneously coupled TG-MS measurements using an atmosphere of 5% H_2 /95% N_2. For WO_3 doped with LiCl, NaCl, and KCl, the release of HCl starts at 347, 506 and 451ºC, respectively. The formation of HCl results from the reaction between the alkali chloride, WO_3, and water. Ubiquitous traces of moisture in the gas are sufficient for reaction with amounts of MCl in WO_3, such as those used in our samples.

For WO_3 doped with LiCl, NaCl and KCl, the reduction of WO_3 starts at 720ºC, 706ºC and 672ºC, distinctly higher temperatures than 579ºC, measured for undoped WO_3 under the same experimental conditions. The alkali tungstates, formed from the

alkali chlorides during the early pre-reduction stages of the process, retard the reduction process of WO_3 and in this way coarsen the tungsten powder.

* * *

The authors thank Matthew J. Connor and Henry J. Stevens for their technical assistance.

References

1 E. Lassner and W.-D. Schubert, Tungsten, Properties, Chemistry, Technology of the Elements, Alloys, and Chemical Compounds, Kluwer, New York 1999, p. 229.
2 W. G. Mallard, Ed., NIST Standard Reference Database Number 69, 2001. (http://webbook.nist.gov/chemistry/)
3 O. Knacke, O. Kubaschewski and K. Hesselman, Thermochemical Properties of Inorganic Substances, 2nd edn., Town, Publisher 1991.
4 J. Qvick, private communication.
5 P. Taskinen, P. Hytönen and M. H. Tikkanen, Scandinavian J. Metallurgy, 6 (1977) 228.
6 R. H. Perry and D. W. Green, Perry's Chemical Engineers' Handbook, McGraw-Hill 1999.
7 O. Glemser and H. Ackermann, Z. Anorg. Allg. Chem., 325 (1963) 281.
8 J. O. Hill (Ed.), For Better Thermal Analysis and Calorimetry, Special edn. of the International Confederation for Thermal Analysis, 3rd edn., University of Rome, 1991.
9 A. Lackner, T. Molinari and P. Paschen, Scandinavian J. Metallurgy, 25 (1996) 115.
10 E. Post, private communication.
11 H.-J. Lunk and S. Hübener, 12th Intern. Plansee Seminar '89, Reutte, Proceedings, Vol. 1, RM 11, p. 133.